

Elasticity profile of an unconsolidated granular medium inferred from guided waves: Toward acoustic monitoring of analogue models

L. Bodet ^{a,*}, X. Jacob ^b, V. Tournat ^c, R. Mourgues ^a, V. Gusev ^d

^a LPG, UMR CNRS 6112, Université du Maine, Le Mans, France

^b Laboratoire P.H.A.S.E., EA 3028, Université de Toulouse III, Toulouse, France

^c LAUM, CNRS, Université du Maine, Le Mans, France

^d LPEC, UMR CNRS 6087, Université du Maine, Le Mans, France

ARTICLE INFO

Article history:

Received 20 April 2010

Received in revised form 6 October 2010

Accepted 9 October 2010

Available online 14 October 2010

Keywords:

Granular media

Guided waves

Analogue modelling

ABSTRACT

The monitoring of materials elastic parameters during geological analogue experiments would highly improve the interpretation of involved processes. It would more particularly help the implementation of joint analytical or numerical analyses. We propose laser-Doppler vibrometry as a probing tool for the systematic characterisation of analogue models. We therefore develop an experimental set-up to record small-scale seismic lines at the surface of an unconsolidated granular medium in laboratory conditions. Pressure-wave first arrival times and surface-wave dispersion are then inverted for a one-dimensional Pressure- and Shear-wave velocity structure. Inferred profiles appear to match previously thoroughly estimated properties of the probed medium, thus validating our approach.

© 2010 Elsevier B.V. All rights reserved.

1. Introduction

Analogue modelling has become a strategic tool to address the physics of geological processes, or their evolution over time. Most studies are based on structural observations and on large scale strain measurements, at the models top surface or through transparent side walls. Such approaches may appear restricting when more quantitative results would help the interpretation of geological observations and geophysical data, or to validate analytical and numerical models (Dahlen, 1990). Moreover, most modelling studies only address the plastic behaviour of materials during the experiments, when the knowledge of their elastic parameters would highly improve the analysis of involved processes (Mastin, 1988; Mourgues & Cobbold, 2006). Several parameters, such as the Poisson ratio, are of importance but can most of the time only be roughly estimated. Recent studies, involving hydraulic fracturing to simulate magmatic sills emplacement (Gressier et al., 2010) or to study hydrocarbon traps integrity (Mourgues et al., in press), have for instance combined analytical models with analogue experiments. In this context, analogue modelling is partly chosen to verify analytical predictions. Such predictions highly depend

on involved materials elastic parameters and should require these characteristics to be controlled before and during the experiments.

In typical geological analogue modelling experiments such as sand wedges for instance, the evolution of the models can be monitored using time-laps photography through transparent side walls. Such measurements, combined with computer-aided line drawing, can provide valuable parameters and help quantify the experimental results (Storti et al., 2000). Completed models are often solidified (using transparent resin, by congelation or by simple wetting) and sliced in order to verify the validity of structural observations and deformation measurements performed from the sides. But such techniques cannot be used during the experiments, thus prohibiting any progressive monitoring of the deformation. However, several countermeasures exist to expose the internal structure of analogue sandbox models. Specifically designed vacuum cleaners can be for instance used in order to perform sequential sectioning of the models during their deformation (Mulugeta & Koyi, 1987; Mulugeta & Koyi, 1992; Koyi, 1995). Additionally, advances in optical techniques and digital imaging methods enable accurate measurements of models topography, or high-resolution strain monitoring (Crave et al., 2000; Adam et al., 2005; Nilforoushan & Koyi, 2007; Adam et al., 2008; Graveleau et al., 2008). It consequently improves model characterisation, but observations remain confined to the material surface. Interestingly, it is, however, possible to quantify models volumetric strain using a laser scanner throughout the experiments (Nilforoushan et al., 2008), thus providing valuable insights on the three dimensional (3D) kinematics of modelled processes. Computed X-ray tomography can be applied on analogue models to obtain 3D images of particular structures (Colletta et al., 1991; Adam et al., 2008). Such

* Corresponding author. Present address: UMR CNRS 7619 Sysiphe, Université Pierre et Marie Curie-Paris 6, case courrier 105, 4 place Jussieu 75252 Paris Cedex 05, France. Tel.: +33 1 44 27 48 26; fax: +33 2 44 27 45 88.

E-mail address: ludovic.bodet@upmc.fr (L. Bodet).

method is, however, technically and economically restricting, and still limits models dimensions or their handling during the experiments.

To overcome these drawbacks, Buddensiek (2009) recently developed a small-scale seismic apparatus, consisting of piezoelectric transducers, which allows noninvasive and high-resolution imaging of sandbox models. This technique indirectly provides an evaluation of material Pressure-wave propagation velocities. However, to obtain good source and receiver coupling, the materials have to be saturated with water in a tank (Sherlock, 1999; Sherlock & Evans, 2001; Buddensiek et al., 2009), and such approach cannot be pursued on most standard analogue models involving dry granular media.

The use of noncontacting ultrasonic measurement techniques, such as laser-Doppler vibrometry, can then be alternatively proposed. Laser-Doppler vibrometers can be used to record, without any contact, particle displacement or velocity at the surface of a sample mechanically excited by a controlled source (in contact or not). This technique proved to be efficient in the physical modelling of seismic-wave propagation at various application scales (Nishizawa et al., 1997; Scales & van Wijk, 1999; van Wijk & Levshin, 2004; van Wijk et al., 2004; Bodet et al., 2005; Campman et al., 2005). The noncontacting character of laser-Doppler vibrometers provides flexibility which, if combined with high density sampling abilities, gives the opportunity to simulate typical seismic prospecting records, in the laboratory. It consequently allows to apply standard signal processing and inversion methods of seismic characterisation on small-scale models (Bodet et al., 2005; Bodet et al., 2009). In this Letter, we propose to reproduce this approach on granular materials commonly used in physical and geological analogue modelling. We address the ability of laser-Doppler experiments in the systematic estimation of analogue models elastic properties. The methodology presented here is developed and validated on an unconsolidated granular medium previously thoroughly characterised in terms of Pressure-wave (P) and Shear-wave (S) 1D velocity profiles with depth (Jacob et al., 2008).

2. Laser-Doppler experiments on an unconsolidated granular medium

2.1. The unconsolidated granular medium

Jacob et al. (2008) recently developed a set of acoustic experiments in order to investigate the elastic properties at very low pressures of an unconsolidated granular packed structure under gravity. In the mechanically free surface vicinity of such material, P- and S-wave propagation velocity ($V_{p,s}$) can be considered as power-law dependent on pressure (Gassmann, 1951), hence on depth (z) when bulk density (ρ) can be assumed constant. The velocity structure of such medium can be modelled as

$$V_{p,s} = \gamma_{p,s} (\rho g z)^{\alpha_{p,s}}, \quad (1)$$

where g is the gravity acceleration, $\gamma_{p,s}$ is a depth-independent coefficient mainly depending on elastic properties of grains, and $\alpha_{p,s}$ is the power-law exponent. This horizontal stratification of the elastic properties induces the upward bending of the acoustic rays (so called 'mirage effect'; Liu & Nagel, 1992) in the near surface of the medium. The combination of this gravity-induced rigidity gradient with the free surface enables the propagation of low velocity guided surface acoustic modes (GSAM). These GSAM, localised near the free surface, consist in shear horizontal (SH-) waves and in polarised in the vertical plane (P-SV) waves. P-SV waves can be considered as a result of interactions between longitudinal (or P-) waves and shear vertical (SV-) waves in inhomogeneous medium, theoretically described for dry granular media by Gusev et al. (2006), Aleshin et al. (2007) and Bonneau et al. (2007), as well as experimentally observed by Jacob et al. (2008) or Bonneau et al. (2008) for instance. The dispersion relations of GSAM can be computed for a given set of the

medium elastic parameters (ρ , $\gamma_{p,s}$ and $\alpha_{p,s}$) (Aleshin et al., 2007). Inversely, when it is possible to measure the GSAM dispersion in a given medium, its parameters can be estimated through an optimisation procedure (Jacob et al., 2008).

Jacob et al. (2008) actually thoroughly measured the dispersion relations of P-SV modes at very low pressures in the vicinity of the surface of a laboratory model. To achieve such measurements, a laser-Doppler vibrometer has been used to record the wavefield generated by a vibrated plate vertically embedded into the granular material. The experiment has been conducted using an important number of acoustic excitations of different frequencies. This procedure provided an extremely accurate description of the dispersion relation, over a wide frequency range (typically 0.5 to 5 kHz). These dispersion measurements were then inverted for γ and α in the framework of GSAM theory, in order to retrieve the medium P- and S-wave velocity profiles with depth. Such procedure is, however, too 'heavy' to be planned in the context of analogue models systematic characterisation. But the results of Jacob et al.'s (2008) study provide an accurate description of this unconsolidated granular medium (Fig. 1a) which can then be used here to validate the methodology we develop in the following.

2.2. Experimental set-up and data

The experiments presented in this Letter are performed on Jacob et al.'s (2008) laboratory model which basically consists of a $80 \times 50 \times 35$ cm plexiglas box, filled up with 20 cm of 150 μm diameter glass beads (Fig. 1b). The granular material is prepared by pouring the glass beads into the container, which is eventually gently shaken. Weight and volume measurements of several samples of the granular medium, as well as of the model itself, lead to a bulk density of approximately 1580 kg m^{-3} . The model density can be assumed constant with depth even if it slightly decreases in the vicinity of the free surface at pressures less than 75 Pa (Jacob et al., 2008). The contribution of such density variation to velocity changes is indeed negligible in comparison with the contribution of the medium elastic modulus variations (Gusev et al., 2006). The experimental set-up, previously developed for the physical modelling of wave propagation (van Wijk et al., 2004; Bodet et al., 2005; Campman et al., 2005; Bodet et al., 2009) is reproduced to simulate a seismic line at the laboratory scale. A laser-Doppler vibrometer is used to record particle velocity at the surface of the medium, which is mechanically excited. The laser beam (of 1 mm diameter and 633 nm wavelength here) reflects off a moving target which Doppler-shifts its frequency. Basically, the Doppler-shift can be interpreted to derive the absolute particle velocity of the moving target without contact. But the technique presented here cannot be considered completely noncontacting. To take advantage of the flexibility of a completely noncontacting measurement, it would be preferable to also use a laser source (the signal is an elastic pulse generated by thermal expansion) in addition to the laser receiver. But the mechanical source partly previously tested and validated by Jacob et al. (2008) is preferred here as a first approach.

The source is a 2 mm diameter stick, vertically attached to a low-frequency (LF) shaker and buried in the granular material. The LF-shaker horizontally excites the stick, generating a short pulse with Gaussian frequency spectrum centred on 1.5 kHz. The laser-Doppler vibrometer scans by 1 mm step the surface of the granular medium and records 300 traces in linear single-channel walkway fashion, parallel to the long edges of the box. Each trace is stacked 100 times and the sample rate is 100 kHz. The recorded wavefield can then be presented as a seismogram (Fig. 2a). Despite multiples reflected from the bottom of the box, and possible multiples reflected from the edges, coherent waves clearly appear. Slow surface guided modes (P-SV) dominate the wavefield with apparent velocities up to 50 m s^{-1} . The early event (P), qualitatively observed with apparent velocities up to 170 m s^{-1} , corresponds to fast guided modes considered as mainly longitudinal by Jacob et al. (2008).

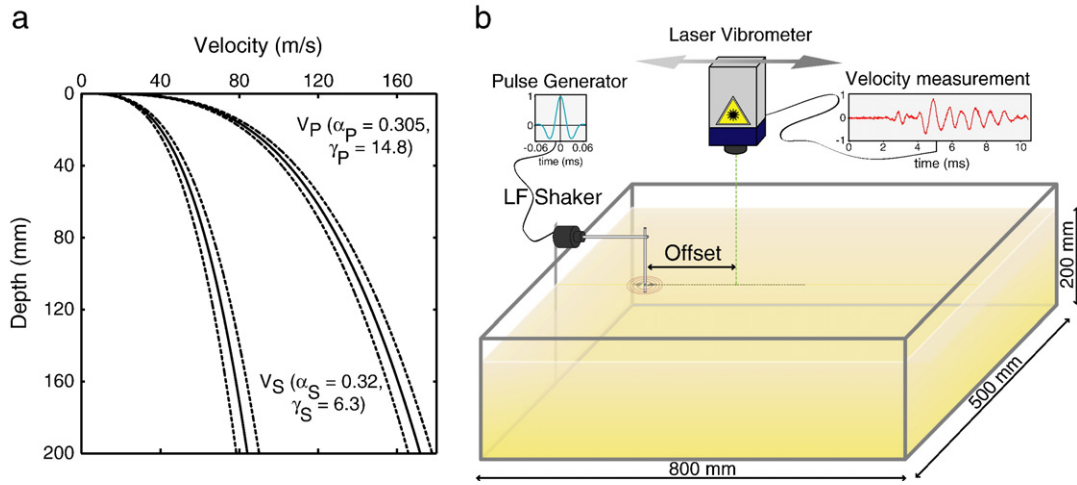


Fig. 1. Laser-Doppler experiments: the unconsolidated granular medium. (a) Velocity models estimated by Jacob et al. (2008), presented with corresponding errors (dashed lines). (b) Experimental set-up developed in the present study.

3. Seismic characterisation of the medium

The P and P-SV events identified on the seismogram are recorded with a good signal-to-noise ratio (greater than 22 dB) up to 300 mm from the source. A more quantitative interpretation can then be easily achieved using typical seismic prospecting techniques. The methodology proposed here consists in analysing P-wave first arrivals and measuring surface-wave dispersion. Traveltimes and dispersion data are then inverted to infer elastic properties of the probed medium, namely P- and S-wave velocity profiles versus depth.

3.1. P-wave velocity model

The P-wave first arrival time is picked at each trace with an estimated error of 5%, providing the experimental traveltime versus offset curve presented on Fig. 3a. It clearly shows a nonlinear increase of traveltime

with source–receiver distance, suggesting an increase of velocity with depth. According to associated wavelengths, ray theory should provide satisfying approximation at all distances and depths, as previously proposed by Bachrach et al. (1998), Bachrach et al. (2000) or Vriend et al. (2007) in the case of unconsolidated sands. Theoretical traveltime versus offset curves can then be calculated for a power-law variation of P-wave velocity with depth (defined by Eq. (1)).

As an illustration, the theoretical P-wave traveltimes in the laboratory model are computed from Jacob et al. (2008) parameters for P-wave velocity ($\gamma_P = 14.8 \pm 0.4$ and $\alpha_P = 0.305 \pm 0.01$, Fig. 3a and b). We use a bulk density of 1580 kg m^{-3} (estimated from several samples of the granular material and from the laboratory model itself) and a gravity acceleration assumed to be 9.81 m s^{-2} . The obtained curve (plain black line on Fig. 3a) clearly fits to picked arrivals within estimated errors (grey shaded area). Conversely, the computation of theoretical traveltimes in the framework of ray theory can be used to invert picked first arrivals for

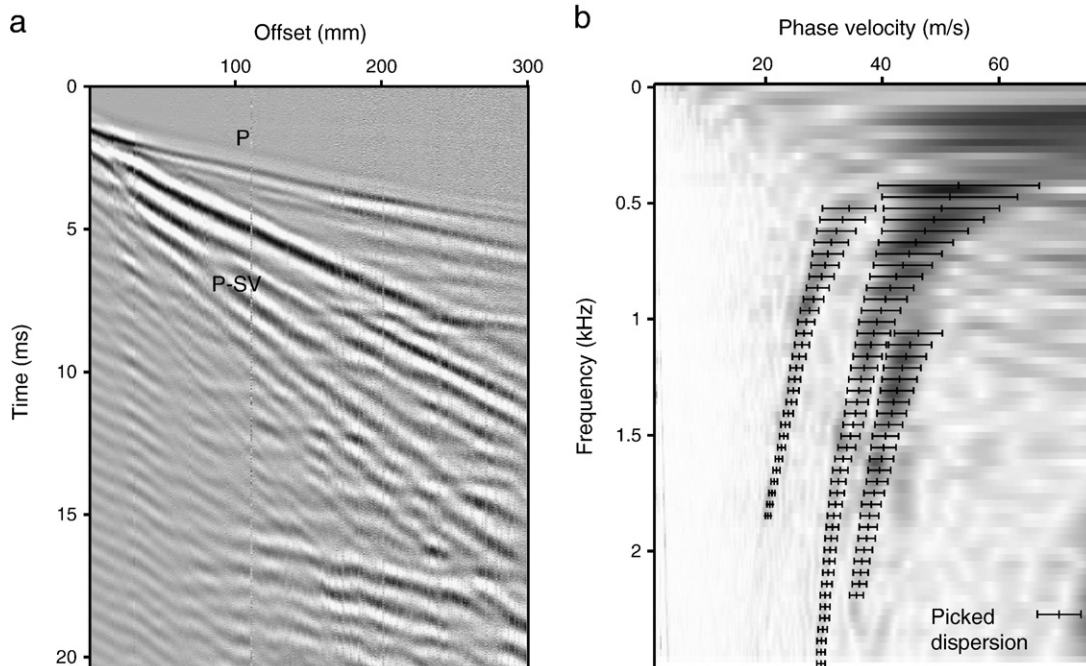


Fig. 2. Laser-Doppler experiments: (a) recorded seismogram of particle velocity, vertical component (300 normalised traces, 1 mm spaced); (b) corresponding normalised dispersion image (linear scale). The maxima (in black) are picked and interpreted as 1st (fundamental), 2nd and 3rd P-SV modes.

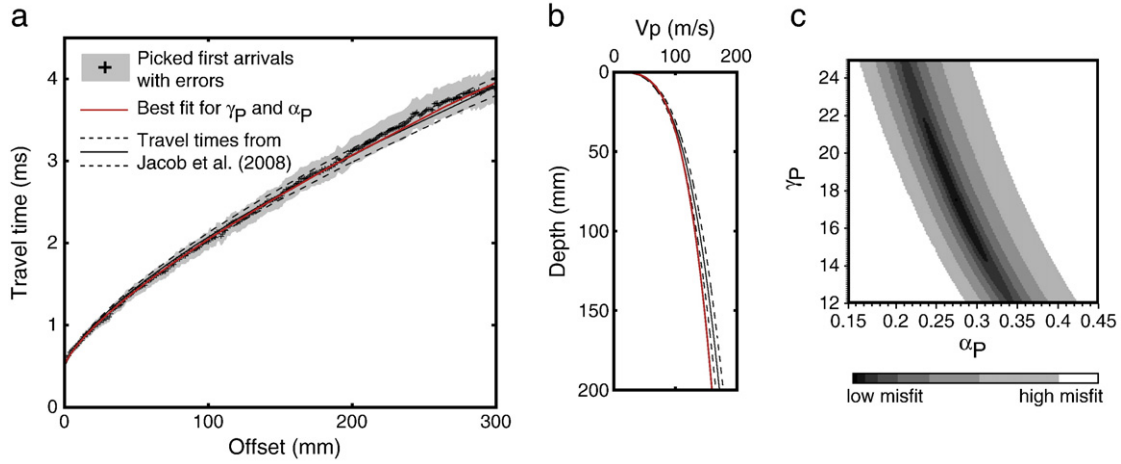


Fig. 3. P-wave first arrival interpretation in the framework of ray theory. (a) Traveltime versus offset plot of picked data within estimated errors (grey shaded area) compared to traveltimes computed from Jacob et al. (2008) model (b) for P-wave velocity within estimated errors (dashed lines). (c) Grid-search inversion of traveltime versus offset for γ_P and α_P : each generated model is depicted by a dot with a grey scale depending on its misfit value. Among 39,411 models, the minimum misfit is obtained for $\gamma_P = 17.5$ and $\alpha_P = 0.275$ (red lines on a and b).

the P-wave velocity structure of the medium. To achieve such inversion, we propose to perform a grid search for γ_P , α_P using the following misfit function:

$$\text{misfit}(\gamma_P, \alpha_P) = \sqrt{\sum_{i=0}^N \frac{(t_{di} - t_{ci})^2}{\sigma_i^2 N}}, \quad (2)$$

where t_{di} and t_{ci} are respectively picked and computed traveltimes at offset x_i . N is the number of traces and σ_i the error in first-arrival time picking at each offset. The grid search is performed with $12 \leq \gamma_P \leq 25$ and $0.15 \leq \alpha_P \leq 0.45$ for a total number of 39,411 models.

The resulting misfit is presented on Fig. 3c. Each generated model is depicted by a dot with a grey scale depending on its misfit value. According to the minimum misfit value, the best fit to data occurs at $\gamma_P = 17.5$ and $\alpha_P = 0.275$. The corresponding traveltime curve and velocity model are shown on Fig. 3a and b, respectively. An important number of models, including (Jacob et al., 2008), exhibit low misfit values around this minimum. These models as well fit to data within estimated errors, suggesting an important uncertainty in the determination of the actual parameters of Eq. (1). According to Jacob et al.'s (2008) parameters, the grid search results indeed show up to 18% error in the estimation of γ_P and to up to 10% error in α_P . Actually, two different (γ_P, α_P) couples can produce very close velocity profiles and lead to close traveltimes (even if the corresponding two power-laws only theoretically cross at one depth below zero). This consequently generates equivalent misfit values according to the standard error in traveltime data. However, if different in terms of model parameters from Jacob et al.'s (2008) estimation, the obtained velocity profile remains satisfying, mainly underestimating velocities at depth (the underestimation being lower than 7%). Such discrepancies between this result and Jacob et al. (2008) could also be explained by the investigation depth of our method. According to the length of the receiver line and taking Jacob et al.'s (2008) model into account, detected rays should have travelled between the surface and a depth of 70 mm. It means that the results of this inversion are only based on shallow material properties and such features show the limits in terms of investigation depth of the method as it is proposed here. A longer receiver line should consequently be used in the future to achieve deeper investigation.

3.2. S-wave velocity model

We analyse the strongly dispersive events observed on Fig. 2a (P-SV), in order to estimate S-wave velocities using surface-wave dispersion inversion technique. Despite several limitations regarding dispersion measurements and inversion process (Socco & Strobbia, 2004; Bodet et al., 2005; O'Neill & Matsuoka, 2005), surface-wave methods can be considered very efficient when strong a priori information about the probed medium is available and thoroughly implemented (Wathelet, 2008). This is the case in the present study since we anticipate a power-law dependence of V_S with depth.

The wavefield dispersion image is computed by a slant-stack in common shot gathers, after correction for geometrical spreading (Fig. 2b). In this plane, the wavefield maxima (in black on Fig. 2b) should correspond to phase velocity dispersion curves of particular P-SV propagation modes. Three modes are identified and extracted with an estimate of error in phase velocity. The maximum wavelength picked is chosen lower than 50% of the spread length (150 mm) in order to avoid near-field effects (Bodet et al., 2009).

Dispersion data are inverted to a 1D-layered velocity model using neighbourhood algorithm (Sambridge, 1999) as implemented by Wathelet et al. (2004) in the framework of surface-wave theory. Assuming a vertically heterogeneous model, theoretical dispersion curves are computed from the elastic parameters using the Thomson–Haskell matrix propagator technique. The neighbourhood algorithm basically performs a stochastic search of the parameter space, namely V_P , V_S , ρ and thickness H of each layer. The parameterisation of the model is achieved here using a single layer overlaying the half-space. The upper layer is a stack of 10 sub-layers following a power-law variation with depth. It is important to note that this number of sub-layers is only a tuning parameter to avoid forward computation instabilities. The half-space depth is of great importance in the parameterisation, since it depends on poorly known depth investigation of the method. A safe first approach is to set the half-space depth equal to 25% of the spread length (Bodet et al., 2005), i.e. 75 mm here. The valid parameter ranges for the sampling of velocity models are 5 to 150 m s⁻¹ for V_S (based on dispersion observations) and 5 to 300 m s⁻¹ for V_P . Density is set as uniform (1580 kg m⁻³) since it is considered of weak constraint on surface-wave dispersion. According to poor influence of P-wave velocity as well, only S-wave velocity profiles are interpreted here. Dispersion data are inverted with 5 distinct and independent runs, generating a total of 25,500 models. The misfit function

is similar to Eq. (2), with t_{di} and t_{ci} being respectively picked and computed phase velocities at frequency f_i . N is the number of frequency samples associated to phase velocity measurements errors σ_i .

Fig. 4a presents all sampled shear-velocity profiles with a misfit lower than 0.7 and their corresponding dispersion curves. Dispersion data (presented with error bars in the inset of Fig. 4a) are well fitted and lowest misfits correspond to S-wave velocity profiles in good agreement with Jacob et al.'s (2008) model. The influence of the half-space depth on the inversion results is then addressed. Anticipating the fact that higher modes should provide greater investigation depths, runs are performed using three deeper half-spaces (100, 125 and 150 mm) for a total number of 102,000 models. Each model, generated with $2 \leq \gamma_s \leq 15$ and $0.15 \leq \alpha_s \leq 0.45$, is depicted on Fig. 4b by a dot with a grey scale depending on its misfit value. According to the minimum misfit value, the best fit to data occurs at $\gamma_s = 5.25$ and $\alpha_s = 0.333$. The estimated power-law exponent correlates well with Jacob et al.'s (2008) model for S-wave ($\gamma_s = 6.3 \pm 0.13$, $\alpha_s = 0.320 \pm 0.006$). The estimated γ_s is, however, lower and leads to an underestimation of velocities at depth, in a similar manner as P-wave velocity results. The underestimation remains lower than 9% at depth so that surface-wave inversion can still be considered satisfying. As far as the probed medium can be considered stratified above the receiver spread, it is possible to overcome such drawback using longer a receiver line (as in the case of P-wave first arrival times inversion).

4. Conclusions

Granular materials are widely used for both geological and physical modelling purpose. Natural sand, granular silica or glass beads provide acceptable analogues in various experiments (e.g. accretionary wedges modelling, gravitational spreading and gliding simulations, hydraulic fracturing studies, hydrogeological modelling, etc.). Such experiments are mostly performed to address the plastic behaviour of studied processes. However, the knowledge of material elastic parameters (before and during the experiments) would highly

help the interpretation of the results. In the context of analytical or numerical analyses associated to analogue modelling studies, the in situ estimation of material elastic parameters would be of great interest as well.

In this Letter, we addressed the ability of laser-Doppler experiments in the seismic characterisation of granular materials involved in analogue modelling. Our methodology has been developed and validated on an unconsolidated granular laboratory medium, perfectly known in terms of Pressure- and Shear-wave 1D velocity profiles with depth. The flexibility and high density sampling abilities of noncontacting measurements made it possible to simulate a small scale seismic line at the surface of the model. We analysed first-arriving P-waves and surface-wave dispersion to infer P- and S-wave velocity profiles versus depth of the laboratory model. Our results correlated well with previously measured velocities of the medium (within errors estimated lower than 9% at depth).

The experimental set-up and methodology presented here proved to be efficient since it provided a velocity structure of the medium in a relative straightforward manner. Its robustness mainly relies on a good a priori knowledge of the model geometry. It can therefore be proposed as a tool for the systematic characterisation of analogue models, more particularly before experiments, when the model structure is well known. The proposed method should be successful as well as a monitoring tool, i.e. to image the evolution of models internal structures. Shear zones for instance, which can be considered as zones of decompaction (due to shearing), will behave as wave reflectors and will thus be detected (Buddensiek, 2009).

To take advantage of the flexibility of a completely noncontacting probing tool, it would be preferable to also use a laser source in addition to the laser receiver. Its use will be considered to achieve 2D reflection seismic profiles, at the laboratory scale. Such technique should be applied using various seismic survey configurations and should give the opportunity to produce seismic images of standard analogue models. Its efficiency can be anticipated in the context of basin-scale tectonic experiments for instance, according to the high contrast between the viscous materials typically used (e.g. silicone

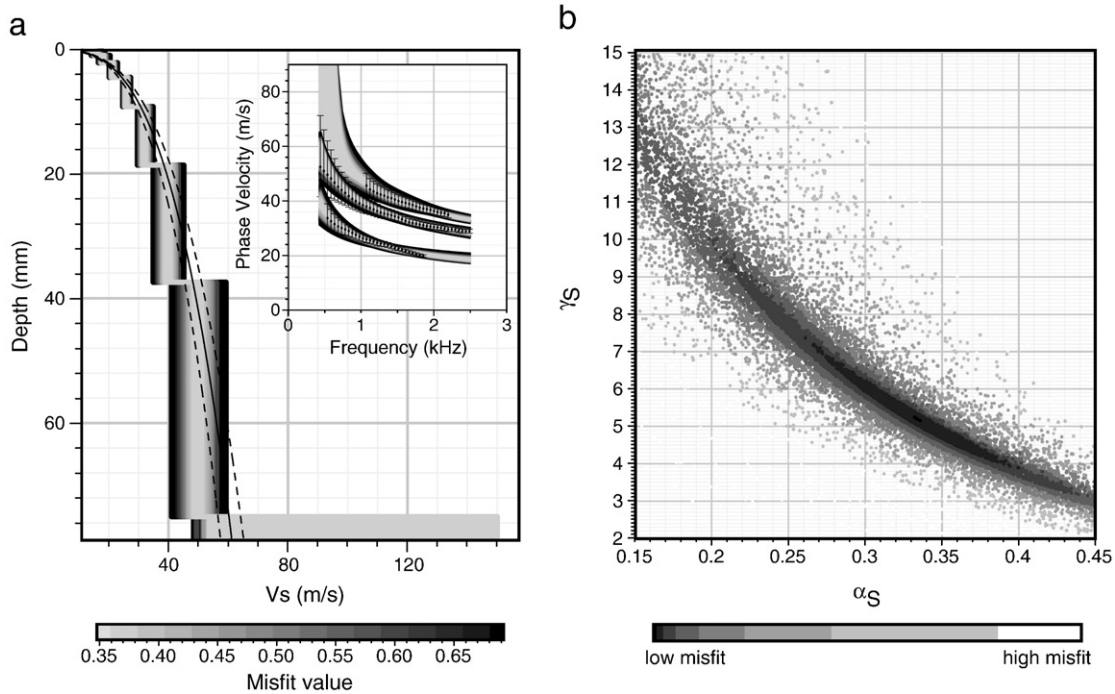


Fig. 4. Dispersion inversion. (a) Inversion performed with a half-space depth of 75 mm: shear-velocity profiles exhibiting misfits less than 0.7 (17,081 models) are presented with corresponding dispersion curves overlaid by experimental dispersion (black dots with error bars). Jacob et al.'s (2008) model for shear-velocity within estimated errors (dashed lines) is given for comparison. (b) Inversion performed with four different half-space depths (75, 100, 125 and 150 mm): each generated model is depicted by a dot with a grey scale depending on its misfit value. Among 102,000 models, the minimum misfit corresponds to $\gamma_s = 5.25$ and $\alpha_s = 0.333$.

putty) and the overlying sand layers (frequently thin compared to the possible investigation depth of the proposed method). Acoustic monitoring combined with the observations from the sides and the top surface could then be proposed to infer the 3D kinematics of modelled processes. Finally, granular materials offer an evident flexibility in terms of models construction and choice of parameters. Their use is then of great interest in the physical modelling of wave propagation to address a wide range of theoretical and practical issues (e.g., heterogeneous media, complex structures, pore fluids, etc.).

Acknowledgments

The authors acknowledge financial support from Région Pays de la Loire, France.

References

- Adam, J., Urai, J.L., Wieneke, B., Oncken, O.H., Pfeiffer, K., Kukowski, N., Lohrmann, J., Hoth, S., van der Zee, W., Schmatz, J., 2005. Shear localisation and strain distribution during tectonic faulting - new insights from granular flow experiments and high resolution optical image correlation techniques. *J. Struct. Geol.* 27, 283–301.
- Adam, J., Schreurs, G., Klinkmueller, M., Wieneke, B., 2008. 2D/3D strain localisation and fault simulation in analogue experiments: insights from X-ray computed tomography, and tomographic image correlation. *Boll. Geofis. Teor. Appl.* 49, 21–22.
- Aleshin, V., Gusev, V., Tournat, V., 2007. Acoustic modes propagating along the free surface of granular media. *J. Acoust. Soc. Am.* 121 (5), 2600–2611.
- Bachrach, R., Dvorkin, J., Nur, A., 1998. High-resolution shallow-seismic experiments in sand: Part II. Velocities in shallow unconsolidated sand. *Geophysics* 63 (4), 1234–1240.
- Bachrach, R., Dvorkin, J., Nur, A., 2000. Seismic velocities and Poisson's ratio of shallow unconsolidated sands. *Geophysics* 65 (2), 559–564.
- Bodet, L., van Wijk, K., Bitri, A., Abraham, O., Côte, P., Grandjean, G., Leparoux, D., 2005. Surface-wave inversion limitations from laser-Doppler physical modeling. *J. Environ. Eng. Geophys.* 10 (2), 151–162.
- Bodet, L., Abraham, O., Clorennec, D., 2009. Near-offsets effects on Rayleigh-wave dispersion measurements: Physical modelling. *J. Appl. Geophys.* 68 (1), 95–103.
- Bonneau, L., Andreotti, B., Clément, E., 2007. Surface elastic waves in granular media under gravity and their relation to booming avalanches. *Phys. Rev. E* 75 (1), 016602.
- Bonneau, L., Andreotti, B., Clément, E., 2008. Evidence of Rayleigh-Hertz surface waves and shear stiffness anomaly in granular media. *Phys. Rev. Lett.* 101 (11), 118001.
- Buddensiek, M.-L., 2009. Seismic imaging of sandbox models. Ph.D. thesis, Freie Universität Berlin.
- Buddensiek, M.-L., Krawczyk, C.M., Kukowski, N., Oncken, O., 2009. Performance of piezoelectric transducers in terms of amplitude and waveform. *Geophysics* 74 (2), T33–T45.
- Campman, X.H., van Wijk, K., Scales, J.A., Herman, G.C., 2005. Imaging and suppressing near-receiver scattered surface waves. *Geophysics* 70 (2), V21–V29.
- Colletta, B., Letouzey, J., Pinedo, R., Ballard, J.F., Bale, P., 1991. Computerized X-ray tomography analysis of sandbox models: examples of thin skinned thrust systems. *Geology* 19, 1063–1067.
- Crave, A., Lague, D., Davy, P., Kermarrec, J., Sokoutis, D., Bodet, L., Compagnon, R., 2000. Analogue modelling of relief dynamics. *Physics and Chemistry of the Earth, Part A. Solid Earth Geod.* 25 (6–7), 549–553.
- Dahlen, F.A., 1990. Critical taper model of fold-and-thrust belts and accretionary wedges. *Annu. Rev. Earth Planet. Sci.* 18 (1), 55–99.
- Gassmann, F., 1951. Elastic waves through a packing of spheres. *Geophysics* 16, 673–685.
- Graveleau, F., Dominguez, S., Malavieille, J., 2008. A new analogue modelling approach for studying interactions between surface processes and deformation in active piedmonts. *Boll. Geofis. Teor. Appl.* 49, 501–505.
- Gressier, J.-B., Mourgues, R., Bodet, L., Mathieu, J.-Y., Galland, O., Cobbold, P.R., 2010. Control of pore fluid pressure on depth of emplacement of magmatic sills: an experimental approach. *Tectonophysics* 489, 1–13.
- Gusev, V., Aleshin, V., Tournat, V., 2006. Acoustic waves in an elastic channel near the free surface of granular media. *Phys. Rev. Lett.* 96, 214301.
- Jacob, X., Aleshin, V., Tournat, V., Leclaire, P., Lauriks, W., Gusev, V.E., 2008. Acoustic probing of the jamming transition in an unconsolidated granular medium. *Phys. Rev. Lett.* 100, 158003.
- Koyi, H., 1995. Mode of internal deformation in sand wedges. *J. Struct. Geol.* 17 (2), 293–300.
- Liu, C.-H., Nagel, S.R., 1992. Sound in sand. *Phys. Rev. Lett.* 68, 2301–2304.
- Mastin, L.G., 1988. Surface deformation and shallow dike intrusion processes at Inyo craters, Long Valley, California. *J. Geophys. Res.* 93.
- Mourgues, R., Cobbold, P., 2006. Sandbox experiments on gravitational spreading and gliding in the presence of fluid overpressures. *J. Struct. Geol.* 28 (5), 887–901.
- Mourgues, R., Gressier, J.-B., Bodet, L., Bureau, D., Gay, A., in press. Basin scale versus localized pore pressure stress coupling - implication for trap integrity evaluation. *Marine and Petroleum Geology*.
- Mulugeta, G., Koyi, H., 1987. Three dimensional geometry and kinematics of experimental piggyback thrusting. *Geology* 15, 1052–1056.
- Mulugeta, G., Koyi, H., 1992. Episodic accretion and strain partitioning in a model sand wedge. *Tectonophysics* 202, 319–333.
- Nilforoushan, F., Koyi, H., 2007. Displacement fields and finite strains in sandbox model simulating a fold-thrust-belt. *Geophys. J. Int.* 169, 1341–1355.
- Nilforoushan, F., Koyi, H., Swantesson, J.O.H., Talbot, C.J., 2008. Effect of basal friction on surface and volumetric strain in models of convergent settings measured by a laser scanner. *J. Struct. Geol.* 30, 366–379.
- Nishizawa, O., Satoh, T., Lei, X., Kuwahara, Y., 1997. Laboratory studies of seismic wave propagation in inhomogeneous media using a laser Doppler vibrometer. *Bull. Seismol. Soc. Am.* 87, 809–823.
- O'Neill, A., Matsuoka, T., 2005. Dominant higher surface-wave modes and possible inversion pitfalls. *J. Environ. Eng. Geophys.* 10 (2), 185–202.
- Sambridge, M., 1999. Geophysical inversion with a neighbourhood algorithm: I. Searching a parameter space. *Geophys. J. Int.* 138, 479–494.
- Scales, J.A., van Wijk, K., 1999. Multiple scattering attenuation and anisotropy of ultrasonic surface waves. *Appl. Phys. Lett.* 74, 3899–3901.
- Sherlock, D.H., 1999. Seismic imaging of sandbox models. Ph.D. thesis, Curtin University of Technology.
- Sherlock, D.H., Evans, B.J., 2001. The development of seismic reflection sandbox modelling. *AAPG Bull.* 85, 1645–1659.
- Socco, L.V., Strobbia, C., 2004. Surface-wave method for near surface characterization: A tutorial. *Near Surf. Geophys.* 2 (4), 165–185.
- Storti, F., Salvini, F., McClay, K., 2000. Synchronous and velocity-partitioned thrusting and thrust polarity reversal in experimentally produced, double-vergent thrust wedges: Implications for natural orogens. *Tectonics* 19, 378–396.
- van Wijk, K., Levshin, A.L., 2004. Surface wave dispersion from small vertical scatterers. *Geophys. Res. Lett.* 31, L20602.
- van Wijk, K., Komatitsch, D., Scales, J.A., Tromp, J., 2004. Analysis of strong scattering at the micro-scale. *J. Acoust. Soc. Am.* 115 (3), 1006–1011.
- Vriend, N.M., Hunt, M.L., Clayton, R.W., Brennen, C.E., Brantley, K.S., Ruiz-Angulo, A., 2007. Solving the mystery of booming sand dunes. *Geophys. Res. Lett.* 34, L16306.
- Wathelet, M., 2008. An improved neighborhood algorithm: Parameter conditions and dynamic scaling. *Geophys. Res. Lett.* 35, L09301.
- Wathelet, M., Jongmans, D., Ohrnberger, M., 2004. Surface-wave inversion using a direct search algorithm and its application to ambient vibration measurements. *Near Surf. Geophys.* 2 (4), 211–221.